

Energy absorption of sand cushions in rockfall impact: Effect of impact angle

Naoto Naito^{1,*} and Kenichi Maeda²

¹Toyohashi University of Technology, 1-1 Hibarigaoka, Tempaku-cho, Toyohashi, Aichi, 441-8580 Japan

²Nagoya Institute of Technology, Gokiso-cho, Showa-ku, Nagoya, Aichi, 466-8555 Japan

Abstract. Energy absorption effects of topsoil and talus in mitigating rockfall impacts should be properly evaluated to design effective countermeasures against rockfalls. However, previous studies have largely focused on scenarios wherein the impact angle is either constant or relatively small; consequently, research on the influence of varying slope gradients, drop angles and impact angles on rockfall energy absorption is limited. To address this gap, this study investigated the rockfall behaviour on horizontal and inclined granular mats through a scaled model and full-scale experiments. The results obtained are summarised as follows: (1) The energy absorption rate of rockfall on granular mats is primarily influenced by the impact angle rather than the slope inclination angle; when the impact angle remains constant, the energy absorption rate is approximately the same regardless of the slope inclination. (2) In full-scale experiments, multivariate analysis of factors such as granular mat thickness, rockfall size, impact velocity, and impact angle revealed that the impact angle had a significant effect on energy absorption. Our study findings deepen the understanding of rockfall behaviour on granular surfaces and provide important insights into the design of rockfall mitigation measures.

1 Introduction

Rockfalls pose significant threats to infrastructure and human safety, making the design of effective mitigation measures crucial. Granular materials, such as topsoil, talus, sand cushions, and gravel cushions, have been shown to play a crucial role in rockfall energy dissipation. These materials function as natural rockfall protection structures and present a fascinating phenomenon from the perspective of granular material mechanics. Understanding the energy absorption mechanisms when rockfalls interact with these granular surfaces is essential for gaining insight into rock behaviour and the dynamic interactions between granular materials and obstacles.

Previous studies have mostly focused on scenarios wherein the impact angle is either constant or relatively small, and research on the influence of varying slope gradients, drop angles and impact angles on rockfall energy absorption is limited [1-5]. Although some studies have been conducted on the effects of impact angles [6-8], few large-scale experimental investigations exist. To address this gap, this study investigated the behaviour of rockfalls on granular surfaces by using both scaled model experiments and full-scale tests. By systematically varying the slope gradient and impact angle, this study aimed to elucidate the influence of these parameters on the energy dissipation during rockfall impacts.

This study builds on existing research by extending the examination of granular material behaviour under

more diverse conditions to provide a deeper understanding of rockfall dynamics and contribute to more effective design strategies for rockfall mitigation. Full-scale and systematic model experiments facilitate more accurate predictions of energy absorption and rockfall behaviour on granular surfaces, potentially yielding valuable insights for engineering applications in rockfall protection.

2 Effects of slope angle and impact angle in scaled model experiments

2.1 Experimental conditions

Oblique incidence of falling rocks was conducted to investigate the effects of the impact angle (the difference between the drop and slope angles) on the rockfall behaviour, as shown in Figures 1 and 2, to examine the kinetic behaviour of falling rocks on inclined surfaces with granular layers [9]. A sphere made of alumina (60 mm in diameter, 408 g in mass, and 3.61 specific gravity) was used as the falling mass, with black dots attached to the surface to calculate the angular velocity, as shown in Figure 3. The impact angle was varied by adjusting the apparatus's inclination angle. The falling rock was released from the positions determined after considering velocity damping to adjust the impact velocity.

* Corresponding author: naoto.naito.xz@tut.jp

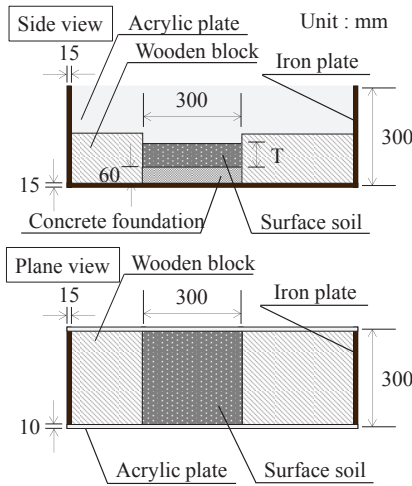


Fig.1. Slope model

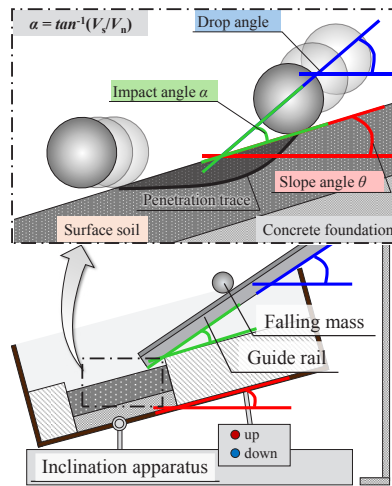


Fig.2. Oblique incidence equipment

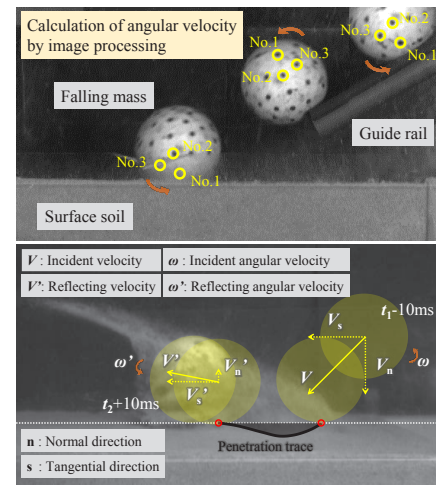


Fig.3. Definition of terms

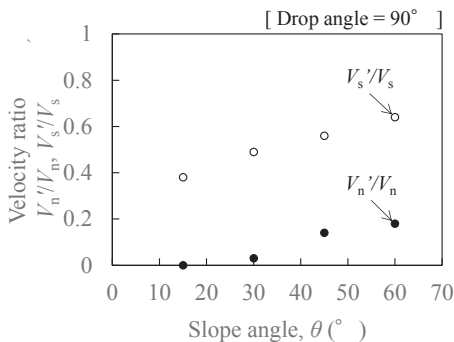


Fig.4. Effects of slope angle on rockfall behaviour

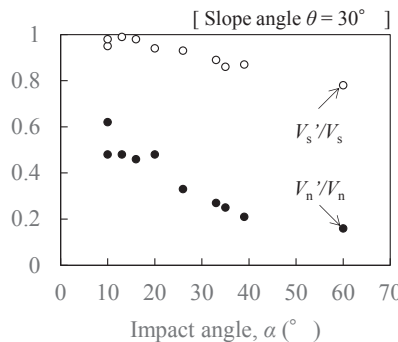


Fig.5. Effects of impact angle on rockfall behaviour

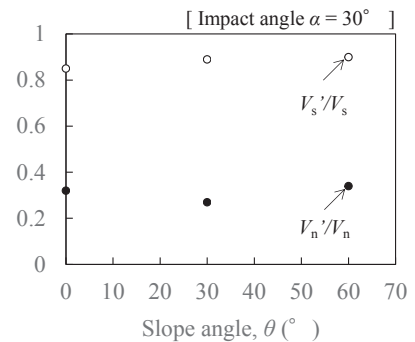


Fig.6. Effects of slope angle and impact angle on rockfall behaviour

Figure 3 depicts the definitions of these terms. Considering the composite velocity in the normal and tangential directions, the velocity of a falling rock is defined as the incident velocity V before impact and the reflection velocity V' after impact. The ratio of the velocities before and after impact is expressed as the velocity ratio, V'/V . The component of velocity in the normal direction is denoted by the subscript n , whereas that in the tangential direction is denoted by the subscript t . For angular velocity, the incident angular velocity before impact is denoted as ω , while the reflection angular velocity after impact is denoted as ω' . The energies of the velocity and rotational components are denoted as E_v and E_r , respectively. The total kinetic energy is denoted as E_k .

Slope surface soil and talus are prone to collapse during rockfall impacts owing to their loosely deposited nature. Therefore, sand with a low shear strength, such that it easily collapses, was used as the experimental sample. Toyoura sand was used as the sediment layer, and the surface soil of the sediment layer remained stable until the rockfall collided, even with variations in the slope angle. The average particle diameter was 0.2 mm. The setup was controlled with a relative density D_r of 70% and moisture content w of 3% to investigate the penetration traces. In this study, the experimental conditions were set based on the ratio of layer thickness T to falling mass diameter D^f .

2.2 Experimental results

Figure 4 shows the results of the experiment conducted with varying slope angles using an inclination apparatus on the sediment layer with a relative layer thickness $T/D^f = 1$. V'_n/V_n and V'_s/V_s represent the velocity ratios in the normal and tangential directions, respectively. The drop condition was vertical free fall with an impact velocity $V = 4.4$ m/s and a ratio of incident rotational energy to incident kinetic energy $E_r/E_k = 0$. Evidently, both the velocity and kinetic energy ratios increased as the slope angle increased. Figure 5 presents the results of an experiment conducted with spheres entering at different impact angles and an impact velocity $V = 4.4$ m/s, with a ratio of incident rotational energy to incident kinetic energy $E_r/E_k = 0.20$ to 0.25 , by using the inclination apparatus on the horizontal sediment layer ($\theta = 0^\circ$) with a relative layer thickness $T/D^f = 1/2$. Evidently, the velocity and kinetic energy ratios decrease as the impact angle increases. Figure 6 shows the results of the experiment conducted with varying slope angles using an inclination apparatus on the sediment layer with a relative layer thickness $T/D^f = 1/2$. The incident conditions were an impact angle $\alpha = 30^\circ$, impact velocity $V = 4.4$ m/s, and a ratio of incident rotational energy to incident kinetic energy $E_r/E_k = 0.20$ to 0.25 . Evidently, the velocity ratio is maintained even when the slope angle increases.

Table 1. Experimental cases

| Reference number | Thickness of sand cushion T (m) | Diameter of falling mass D^f (m) | Impact angle α (°) | Impact velocity V (m/s) | Rotational energy ratio E_r / E_v | Energy absorption ratio $(1 - E_k') / E_k$ |
|------------------|-----------------------------------|------------------------------------|---------------------------|---------------------------|-------------------------------------|--|
| [10] | 1.2 | 1.12 | 24.1 | 17.2 | 0.173 | 69.1 |
| [10] | 1.2 | 0.96 | 41.7 | 18.3 | 0.164 | 77.6 |
| [10] | 0.9 | 1.12 | 36.7 | 17.2 | 0.156 | 63.3 |
| [10] | 0.9 | 1.12 | 42.8 | 18.1 | 0.146 | 67.8 |
| [10] | 0.9 | 0.96 | 32.6 | 17.3 | 0.120 | 70.9 |
| [10] | 0.9 | 0.96 | 27.0 | 15.7 | 0.167 | 63.0 |
| [10] | 0.6 | 1.12 | 39.8 | 18.3 | 0.149 | 63.1 |
| [10] | 0.6 | 0.96 | 44.2 | 18.3 | 0.110 | 60.8 |
| [10] | 0.6 | 0.96 | 37.7 | 18.6 | 0.183 | 57.3 |
| [10] | 0.6 | 0.51 | 40.9 | 18.4 | 0.172 | 71.0 |
| [10] | 0.3 | 0.96 | 44.3 | 18.4 | 0.191 | 56.0 |
| [11] | 0.3 | 0.51 | 35.6 | 15.4 | 0.226 | 55.2 |
| [11] | 0.6 | 1.12 | 29.8 | 13.7 | 0.149 | 45.6 |
| [11] | 0.6 | 1.12 | 41.1 | 14.0 | 0.115 | 89.5 |
| [11] | 0.6 | 1.12 | 46.2 | 15.4 | 0.221 | 81.6 |
| [11] | 0.6 | 1.12 | 36.2 | 16.1 | 0.153 | 73.8 |
| [11] | 0.6 | 1.12 | 35.9 | 17.6 | 0.131 | 65.9 |
| [11] | 0.6 | 1.12 | 42.3 | 14.6 | 0.185 | 78.6 |
| [11] | 0.6 | 0.51 | 48.3 | 20.1 | 0.128 | 85.1 |

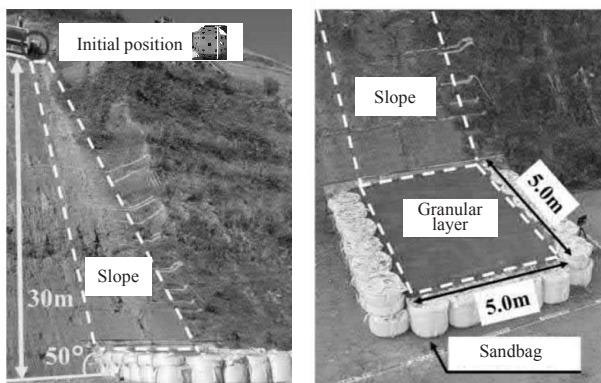


Fig.7. Full-scale experiments setup

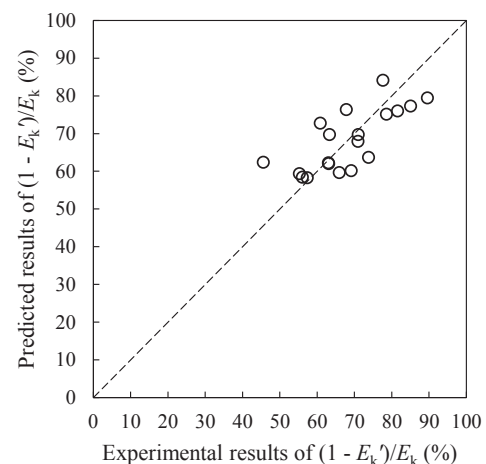


Fig.8. Comparison of experimental and predicted results of the energy absorption ratio

3 Multivariate analysis of impact conditions in full-scale experiments

3.1 Experimental conditions

This study analysed the results of the full-scale rockfall experiments on sand cushions conducted by Isoai et al [10,11]. Figure 7 shows the full-scale experimental setup. Table 1 lists the experimental cases analysed. The experiments involved dropping a weight, whose shape complies with the European Organisation for Technical Assessment standards [12], from a 50° slope, causing it to collide with a sand cushion. The sand cushion layer thicknesses were 0.3, 0.6, 0.9, and 1.2 m, and the weights had masses of 250, 1600, and 2500 kg.

3.2 Analysis results

A multiple regression analysis was performed with explanatory variables, including the sand cushion layer

thickness T , weight diameter D^f , impact angle α , impact velocity V , rotational energy ratio E_r/E_k , and rockfall energy absorption rate E_k'/E_k by the sand cushion as the objective variable, where E_k' represents the reflected kinetic energy after the sand cushion impact. The following regression equation was derived:

$$E_k'/E_k = 30.42 T - 12.70 D^f + 1.418 \alpha - 3.169 V - 59.34 E_r/E_k + 68.41 \quad (1)$$

Here, the dependent variable and equation constants represent the regression coefficients and the constant term. Figure 8 depicts the experimental rockfall energy absorption rates and the predicted values based on the regression equation, and the regression equation was consistent with the experimental results. Using this regression equation, the influence of sand cushion layer thickness (0.3–1.3 m), weight diameter (0.5–1.3 m),

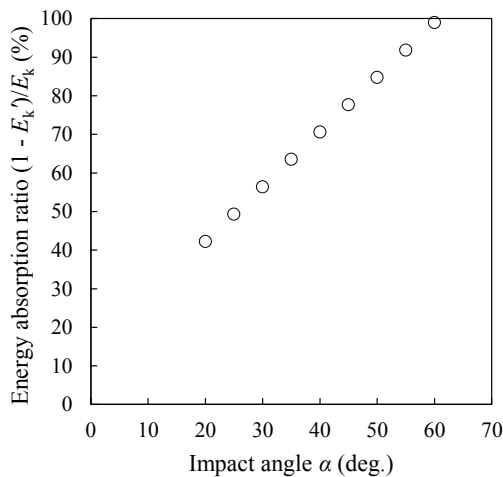


Fig.9. Predicted results based on the multiple regression equation

impact angle (20°–60°), impact velocity (5–30 m/s), and rotational energy ratio (0.1–0.2) on energy absorption rates was investigated. The results showed that the most influential variable was the impact velocity, followed by the impact angle. Figure 9 shows the predicted results based on the regression equation for impact velocity, indicating that when the impact angle is 60°, more than 90% of the rockfall energy can be absorbed.

4 Conclusion

This study investigated rockfall behaviour on granular surfaces through scaled model experiments and full-scale tests, systematically varying the slope gradient, drop angle and impact angle to elucidate their influence on energy dissipation during impacts.

The study results revealed that the energy absorption rate was more strongly influenced by the impact angle than by the slope angle. Furthermore, multiple regression analysis of the full-scale experiments confirmed the significant effect of the impact angle on energy absorption. The findings of this study deepen the understanding of rockfall behaviour on granular surfaces and afford important insights into the design of rockfall mitigation measures.

Future research will seek to clarify the cushioning mechanism of granular mats, wherein the impact angle is the dominant factor, through numerical analysis methods such as the discrete element method.

This study was supported by the Japan Society for the Promotion of Science (Grant-in-Aid for Young Scientists 23K13402 and Scientific Research (B) 23H01501).

References

1. K.T. Chau, R.H.C. Wong, J.J. Wu, Coefficient of restitution and rotational motions of rockfall impacts, *Int. J. Rock. Mech. Min. Sci.*, **39**:69-77 (2002) [https://doi.org/10.1016/S1365-1609\(02\)00016-3](https://doi.org/10.1016/S1365-1609(02)00016-3)

2. V. Labiouse, B. Heidenreich, Half-scale experimental study of rockfall impacts on sandy slopes, *Nat. Hazard.*, **9**(6):1981–1993.(2009) <https://doi.org/10.5194/nhess-9-1981-2009>
3. C. Zhu, D. Wang, X. Xia, Z. Tao, M. He, C. Cao, The effects of gravel cushion particle size and thickness on the coefficient of restitution in rockfall impacts. *Nat. Hazards Earth Syst. Sci.* **18**:1811–1823. (2018) <https://doi.org/10.5194/nhess-18-1811-2018>
4. B. Garcia, V. Richefeu, J. Baroth, D. Daudon, P. Villard, Collision of shaped boulders with sand substrate investigated by experimental, stochastic, and discrete approaches. *J. Geophys. Res. Earth. Surf.* (2020) <https://doi.org/10.1029/2019JF005500>
5. S.Z. Duan, G.L. Li, X. Yang, X.R. Wei, Predicting the velocity and trajectory of a rockfall after collision considering the effects of slope properties, *Nat. Hazards*, **120**: 2057–2072 (2024) <https://doi.org/10.1007/s11069-023-06278-2>
6. P. Asteriou, Effect of Impact Angle and Rotational Motion of Spherical Blocks on the Coefficients of Restitution for Rockfalls, *Geotech. Geol. Eng.*, **37**, 2523–2533. (2019) <https://doi.org/10.1007/s10706-018-00774-0>
7. J. Tang, X. Zhou, K. Liang, Y. Lai, G. Zhou, J. Tan, Experimental study on the coefficient of restitution for the rotational sphere rockfall, *Environ. Earth Sci.*, **80**, 419. (2021) <https://doi.org/10.1007/s12665-021-09684-6>
8. S. Duan, H. Yu, B. Xu, Numerical simulation of a rockfall impacting a gravel cushion with varying initial angular velocity and particle sizes, *Granular Matter*, **25**, 33. (2023) <https://doi.org/10.1007/s10035-023-01320-3>
9. N. Naito, K. Maeda, Y. Ushiwatari, K. Suzuki, R. Kawase, Rock fall behaviors on inclined granular mats with different impact conditions, *Journal of Structural Engineering*, **62A**:1031-1042. (2016) (in Japanese) <https://doi.org/10.11532/structcivil.62A.1031>
10. R. Isoai, K. Maeda, N. Sugiyama, M. Sugawara, H. Konno, N. Naito, Full-scale weight-impact test for evaluating the rockfall energy absorption effect of the sand cushion and 2D-DEM analysis, *Journal of Structural Engineering*, **68A**:999-1012.(2022) (in Japanese) <https://doi.org/10.11532/structcivil.68A.999>
11. R. Isoai, K. Maeda, Y. Ushiwatari, T. Nakamura, A. Kimura, Full scale weight-impact test of rockfall protective soil embankment with sand cushion in the pocket, *Journal of Structural Engineering*, **69A**:1082-1094.(2023) (in Japanese) <https://doi.org/10.11532/structcivil.69A.1082>
12. European Organization for Technical Approvals, Guideline for European Technical Approval of Falling Rock Protection Kits, p.38. (2013) <https://www.eota.eu/sites/default/files/uploads/ETAGs/etag-027-april-2013.pdf>